

## A Modified Navigation Technique for Formation Control of Sonar-Equipped Mobile Robots with Large Obstacle Avoidance

Atsushi Fujimori<sup>1</sup>, Atsushi Hosono<sup>2</sup>, Kazuro Takahashi<sup>2</sup> and Shinsuke Oh-hara<sup>3</sup>

<sup>1</sup>Professor, Department of Mechanical Engineering, University of Yamanashi, Japan.

<sup>2</sup>Student, Department of Mechanical Engineering, University of Yamanashi, Japan.

<sup>3</sup>Assistant Professor, Department of Mechanical Engineering, University of Yamanashi, Japan.

Corresponding Author: Atsushi Fujimori

**ABSTRACT:** This paper presents a formation control of multiple mobile robots with large obstacle avoidance. The mobile robots considered in this paper have multiple sonars which are used for not only constructing formation but also avoiding obstacle. The novel modules overcoming the drawbacks of the previous navigation algorithm [12] are introduced to accomplish the obstacle avoidance and formation control. The effectiveness of the proposed techniques are examined by an experiment using three mobile robots.

**KEY WORDS:** Obstacle avoidance, Formation control, Leader-follower method, Sonar assignment

Date of Submission: 16-01-2019

Date of acceptance: 28-01-2019

### I. INTRODUCTION

In recent, formation control of multiple mobile robots has been one of great attentions in robotic society over the past decades because multiple robotic systems contain potentials for accomplishing tasks which are more than single robotic systems can manage; for example, payload/object transportation, exploration, surveillance, search and rescue and mapping of unknown or partially unknown environments. Multiple robots may be required to make a formation for accomplishing those tasks [1] - [8]. The authors have studied the formation control of mobile robots which equip multiple sonars [9]-[12]. The formation control approach adopted in our studies is based on the leader-follower technique [1], [3], [4]. In [9], a distributed control law, called self-made input (SMI), was proposed in the frame of the leader-follower technique. The formation control with an obstacle avoidance was successfully performed by combining the SMI with a reactive collision avoidance method [12]. Since the size of obstacles considered in [12] was almost the same as that of the mobile robots, the time length required for avoiding the obstacle was short; that is, the quantity of avoidance was small. When the size of obstacles is large, the technique used in [12] was not well worked because the amount of avoidance is large. Therefore, further consideration and/or additional techniques are needed.

The aim of this paper is to propose a navigation technique of formation control with a large obstacle avoidance. Based on the technique in the previous study [12], this paper proposes the following modules to overcome the drawbacks in the previous study. First, the shape of the formation is changed to accomplish obstacle avoidance surely. After avoiding the obstacle, the shape of the formation is re-constructed to the original one. Furthermore, some modules are newly introduced to assist the existing modules in the previous navigation algorithm. The effectiveness of the proposed techniques is examined in experiments using three mobile robots.

### II. FORMATION CONTROL AND OBSTACLE AVOIDANCE

This section presents the statements of problem of formation control based on the leader-follower technique, mobile robots used in the experiment and the navigation algorithm in the previous study [12].

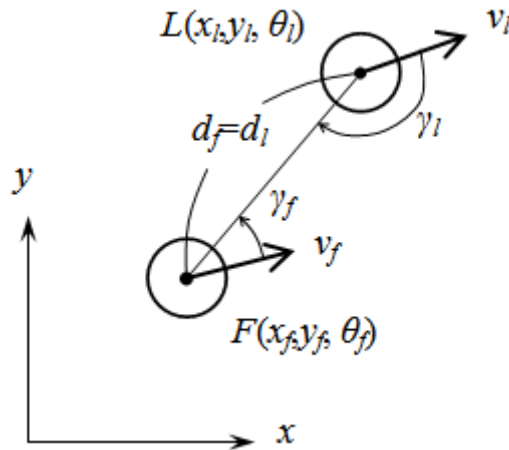


Figure 1: Relative position and relative orientation between leader and follower robots

### II.A. Formation Control by Leader-Follower Method

Consider a mobile robot which moves on the two-dimensional plane. The position of the robot is represented by the fixed Cartesian coordinates  $(x(t), y(t))$  where  $t$  is the continuous-time. The directional angle of the robot is  $\theta(t)$  ( $-\pi \leq \theta(t) < \pi$  [rad]), which is measured from the positive  $x$ -axis. The linear and the angular velocities are respectively  $v(t)$  and  $\omega(t)$  which are the control commands to the mobile robot. The equation of kinematics of the mobile robot is given by

$$\begin{cases} \dot{x}(t) = v(t) \cos \theta(t) \\ \dot{y}(t) = v(t) \sin \theta(t) \\ \dot{\theta}(t) = \omega(t) \end{cases} \quad (1)$$

The magnitudes of the control commands are constrained as

$$|v(t)| \leq v_{\max}, \quad |\omega(t)| \leq \omega_{\max} \quad (2)$$

where  $v_{\max}$  and  $\omega_{\max}$  are the maximum values of  $v(t)$  and  $\omega(t)$ , respectively.

Figure 1 shows a leader-follower formation control of two mobile robots, where  $L$  is the leader robot while  $F$  is the follower robot [1], [4]. Hereafter, the subscript  $l$  and  $f$  in the notations mean the leader and the follower robots, respectively. The equations of both robots are given by Eq. (1) whose variables are replaced to their own state and input variables. The relative distance between the leader and the follower robots is denoted as  $d_l (=d_f)$  and the relative angles from their heading are denoted as  $\gamma_l$  and  $\gamma_f$ , respectively. The objective of the formation control by the leader-follower technique is to navigate multiple mobile robots from start to goal with keeping a formation and without colliding any obstacles. In the concrete, the follower robot is controlled by keeping  $(d_f, \gamma_f)$  to their references  $(d_f^{ref}, \gamma_f^{ref})$  which are specified in advance. The equations of the relative distance and the relative angle include the states and the control commands with respect to both the leader and the follower robots. To realize the formation control by means of a distributed manner, Fujimori et al. [9] proposed a follower control law, called self-made input (SMI), in which the follower input  $v_f$  and  $\omega_f$  were given by the state of the follower robot and the estimates of the leader robot. The SMI does not need any communication tool between the leader and the follower robot. This paper uses the SMI for the formation control law.

### II.B. Mobile Robot Pioneer

Figure 2 shows photos of Pioneer-1 and -2 [13] - [15] which are used for formation control in this study. The size of Pioneer-1, shown in the left and the middle photos, is 450 [mm] from stem to stern, 360 [mm] between the left and right wheels, and 225 [mm] to the top. The size of Pioneer-2, shown in the right photo, is almost the same as that of Pioneer-1. The drive system of Pioneer-1 and -2 is powered by two reversible DC motors. Each drive motor includes an optical encoder for position sensing. Pioneer-1 has seven ultrasonic sonar transducers. The sonars are attached to the front and both sides. While Pioneer-2 has eight ultrasonic sonar transducers. Table I shows the attached angles of the sonars from the forward direction of Pioneer-1 and -2, respectively.



Figure 2: Pioneer-1 and -2

Table I: Attached angles of sonars in Pioneer-1 and -2

No. of sonar <i>i</i>	$\varphi_i$ [deg]	
	Pioneer-1	Pioneer-2
0	90	90
1	30	50
2	15	30
3	0	10
4	-15	-10
5	-30	-30
6	-90	-50
7	-	-90

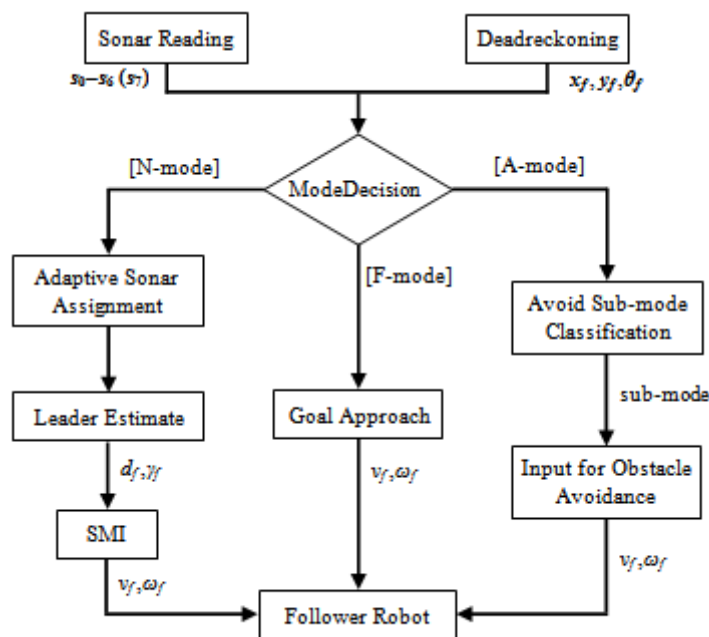


Figure 3: Signal process from sonar reading and deadreckoning to control commands of follower robot presented in [12] (previous navigation algorithm)

The multiple sonars are used not only to detect an obstacle for collision avoidance but also to track the leader robot for constructing formation. Letting  $s_i$  be the output of the  $i$ -th sonar and  $\varphi_i$  be the attached angle of the  $i$ -th sonar,  $d_f$  and  $\gamma_f$  are then calculated by averaging the outputs of the fired sonars with the weighting coefficient  $w_i$  of the  $i$ -th sonar [12]; that is,

$$d_f = \frac{\sum_{i \in \Phi} w_i s_i}{\sum_{i \in \Phi} w_i}, \quad \gamma_f = \frac{\sum_{i \in \Phi} w_i \varphi_i}{\sum_{i \in \Phi} w_i} \quad (3)$$

where  $\Phi$  is the set of the specified sonars number which sonars are used for determining  $d_f$  and  $\gamma_f$ . The details are described in [12].

### II.C. Obstacle Avoidance

A reactive obstacle avoidance technique which was given in [12] is also used in this study. The process mentioned in [12] summarized as follows. According to the fired sonars which detect an obstacle within the specified range, the obstacle avoidance aspects are classified into eight categories; *Front*, *Left*, *Right*, *Front-Left*, *Front-Right*, *Left-Front-Right*, *Left-Right* and *Back*. These are called the sub-modes in the collision avoidance. The control commands of the follower robot  $v_f$  and  $\omega_f$  are then given according to the sub-modes. Combining the SMI for the formation control with the reactive obstacle avoidance, a flowchart of signal process to generate the control commands of the follower robot ( $v_f$  and  $\omega_f$ ) is shown in Fig. 3[12]. Using the outputs of sonars and the deadreckoning information, one of three modes is selected at Mode Decision, where N-mode means the formation control, A-mode means the obstacle avoidance and F-mode is the final navigation in which the mobile robots approach to the goal and their velocities are decreased.

### III. CONTROL STRUCTURE FOR LARGE OBSTACLE AVOIDANCE

This section presents a new navigation algorithm of formation control. First, problems when the previous navigation algorithm Fig. 3 is applied to the formation control with large obstacle avoidance are mentioned. Thenew navigation algorithm including novel modules is then proposed to overcome the problems.

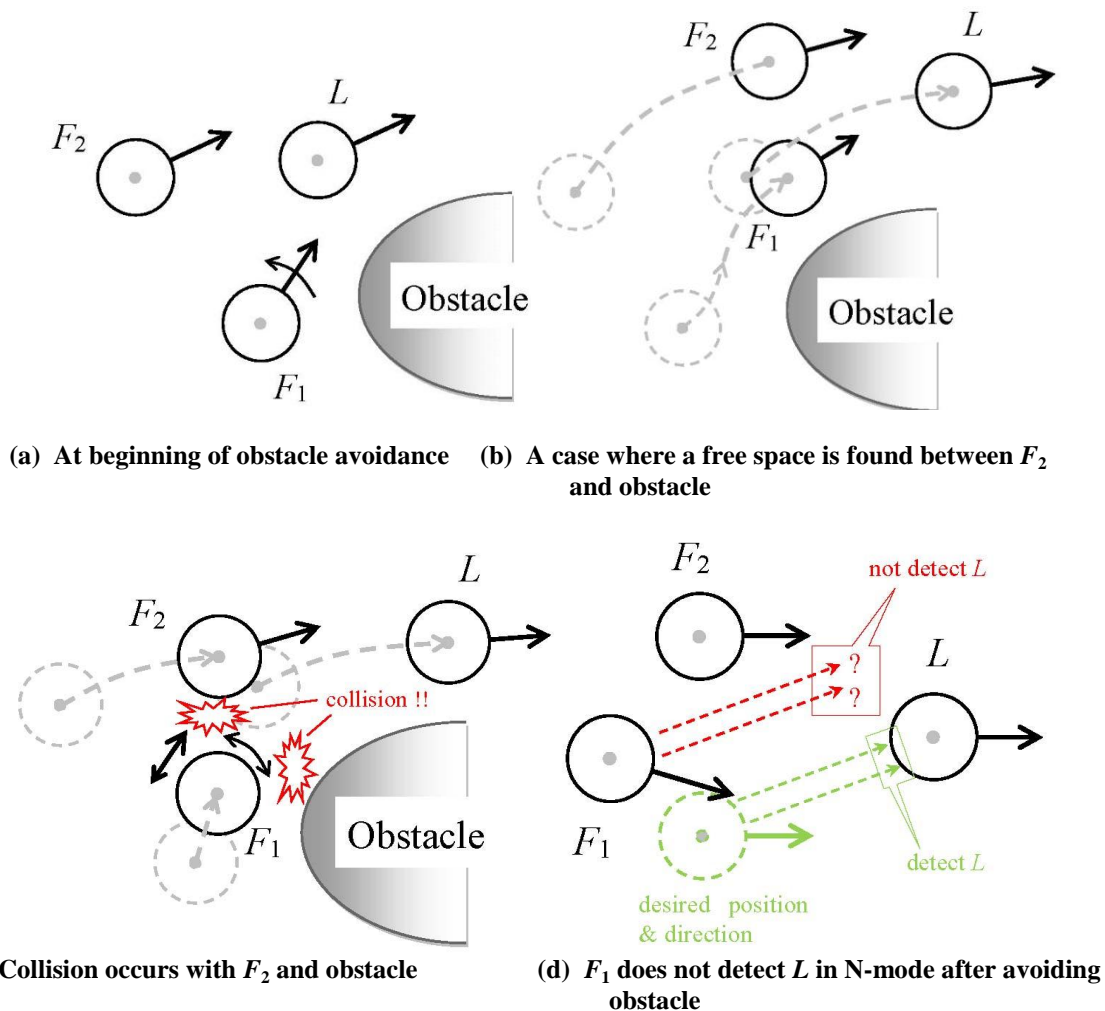


Figure 4: Aspects of formation control with a large obstacle avoidance by navigation algorithm [12]

### III.A. Problems in Previous Algorithm

Figure 4 show aspects that three mobile robots avoid an obstacle with keeping a triangle formation where  $L$  is the leader robot, and  $F_1$  and  $F_2$  are the follower robots. Figure 4(a) shows an aspect that  $L$  almost finishes avoiding the obstacle and  $F_1$  begins to avoid the obstacle by changing its direction to the left. This action may bring a collision with  $F_2$ .  $F_1$  is easy to become the so-called "dead-rock" in which any free space cannot be found in the front of  $F_1$ . As shown in Fig. 4(b), when  $F_1$  fortunately finds free space between  $F_2$

and the obstacle, the obstacle avoidance of  $F_1$  is succeeded with keeping the formation. On the other hand, in the case of Fig. 4(c), if  $F_1$  did not find a enough free space in the front, then  $F_1$  does not avoid the obstacle or misses  $L$ ; that is, the formation control is failed. As another failed case, Fig. 4(d) shows that  $F_1$  is not able to detect  $L$  after avoiding the obstacle and returning to the original formation. This case is happened that the sonars for tracking the leader robot are not suitably assigned or the positions of the leader are not acceptably estimated.

### III.B. Proposed Navigation Algorithm

To overcome the problems mentioned in the previous subsection, Fig. 5 shows the flow chart of the proposed navigation algorithm including the new modules. The modules used in Fig. 3 are also included in Fig. 5. On limitation of the space, the descriptions of F-mode are omitted. The following three points are mainly introduced in the proposed navigation algorithm; (i) N-mode is divided into three sub-modes; N-f-mode, N-r-mode and N-s-mode by the judgement *Nav Select*. (ii) *Form Change* is inserted at the beginning of A-mode. (iii) *Sonar Prediction* and *Move Prediction* are added to assist *Adaptive Sonar Assignment* and *Leader Estimate*, respectively. As far as (iii) is concerned, the dashed lines in Fig. 5 means the exchanges of the information which is updated in each module when the mode is switched. The rest of this subsection explains these new modules in the discrete-time representation.  $t_k$  means the  $k$ -th sampling time where the sampling time is given by  $T_s$ .

1) *N-s-mode*: In the reactive obstacle avoidance method, the mode is decided by the sonar output situation in time. When the mode returns to N-mode from A-mode, there may be the situation that the obstacle avoidance is not accomplished enough. In this case, A-mode is immediately selected again; that is, the follower robot falls into an unstable movement in which A-mode and N-mode are repeated. To avoid this, the previous control commands are maintained when the follower robot comes back to N-mode from A-mode in a while. It is managed by *Keep Command*.

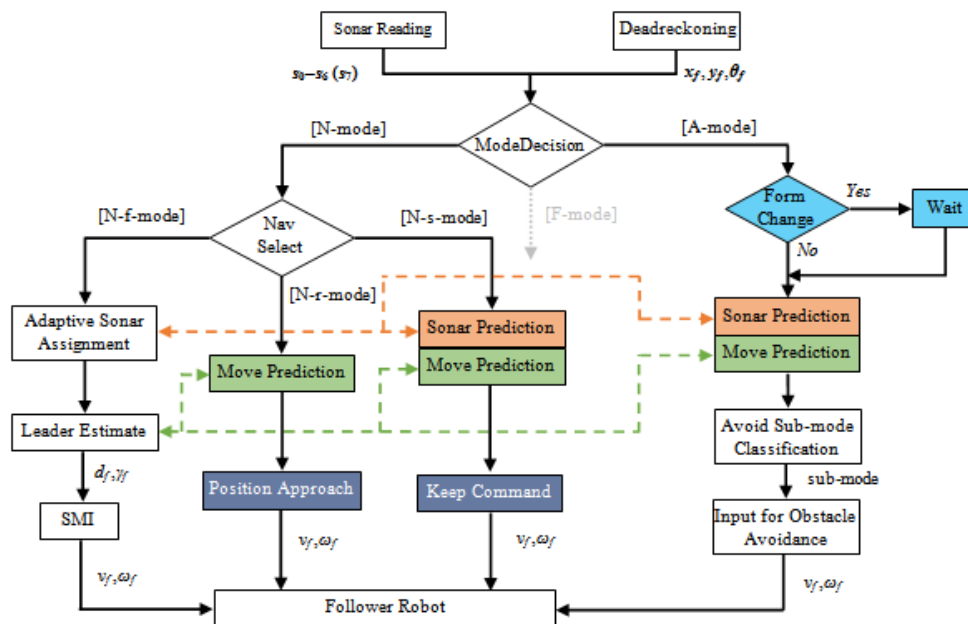


**Figure 5: Flow chart of proposed navigation algorithm**

2) *Form Change*: It is necessary for large-sized obstacles that the obstacle avoidance is surely accomplished as the priority. The shape of the formation is then changed to a suitable shape for avoiding the obstacle. In the case of Fig. 4(c), the formation shape of the follower robot  $F_1$  should be changed to align formation shape; that is, the leader of  $F_1$  is changed to  $F_2$ , the references for the new formation shape and the number of the sonars for tracking the leader robot are changed. As another technique, *Wait* module is inserted at the beginning of *Form Change* to avoid the collision with  $F_2$  and obtain an sufficient free space between them. After  $F_1$  waited in a while,  $F_1$  follows  $F_2$  in the line formation shape.

3) *Sonar Prediction*: After the mode returns from A-mode to N-mode, the sonars for tracking the leader robot may be not suitable because the direction of the follower robot was varied due to the obstacle avoidance behaviors in A-mode. *Sonar Prediction* is then introduced to adjust the number of sonars for tracking the leader robot in A-mode and N-s-mode. Consider a case that the mode is switched to N-s-mode or A-mode at

the discrete-time  $t_{k1}$ . Letting  $n_u(t_k)$  and  $n_l(t_k)$  be the upper and the lower number of the sonars for tracking the leader robot at the discrete-time  $t_k$ , the followings are defined for  $k > k_1$ :

$$\Delta n(t_k) \square n_u(t_k) - n_l(t_k) \tag{4}$$

$$\Delta \theta(t_k) \square \theta_f(t_k) - \theta_f(t_{k1-1}) \tag{5}$$

$\Delta n(t_k)$  is the difference of the sonar numbers and  $\Delta \theta(t_k)$  is the amount of direction angle change from the mode switch.  $n_u(t_k)$  and  $n_l(t_k)$  are then shifted by comparing  $\Delta \theta(t_k)$  with the attached angle of the sonars  $\varphi_i$ . The algorithm for Pioneer-1 is shown in the following.

```

if ( $\Delta \theta(t_k) \geq \varphi_2$ ) & ( $\Delta \theta(t_k) < \varphi_1$ ),  $n_u(t_k) = n_u(t_{k-1}) + 1$ 
else if ( $\Delta \theta(t_k) \geq \varphi_1$ ) & ( $\Delta \theta(t_k) < \varphi_0$ ),  $n_u(t_k) = n_u(t_{k-1}) + 2$ 
else if ( $\Delta \theta(t_k) \geq \varphi_0$ ),  $n_u(t_k) = n_u(t_{k-1}) + 3$ 
 $n_l(t_k) = n_u(t_k) - \Delta n(t_k)$ 
if ( $\Delta \theta(t_k) \leq \varphi_4$ ) & ( $\Delta \theta(t_k) > \varphi_5$ ),  $n_l(t_k) = n_l(t_{k-1}) - 1$ 
else if ( $\Delta \theta(t_k) \leq \varphi_5$ ) & ( $\Delta \theta(t_k) > \varphi_6$ ),  $n_l(t_k) = n_l(t_{k-1}) - 2$ 
else if ( $\Delta \theta(t_k) \leq \varphi_6$ ),  $n_l(t_k) = n_l(t_{k-1}) - 3$ 
 $n_u(t_k) = n_l(t_k) + \Delta n(t_k)$ 
    
```

**4) Move Prediction:** It is important for formation control to catch the position of the leader robot. The position of the leader robot is estimated by using the output of the sonars for tracking leader in *Leader Estimate*. Since *Leader Estimate* is in N-f-mode, the estimation does not perform in other modes. To assist the position estimation, *Move Prediction* is introduced to predict the position of the leader robot in the A-mode, N-s-mode and N-r-mode. It is predicted by supposing that the leader robot moves straight with the normal linear velocity  $v_0$ . Consider a case that the mode is switched to N-s-mode, N-r-mode or A-mode at the discrete-time  $t_{k2}$ . It was N-f-mode at  $t_{k2-1}$ . Then, using the estimated position of the leader robot  $(\hat{x}_l(t_{k2-1}), \hat{y}_l(t_{k2-1}), \hat{\theta}_l(t_{k2-1}))$ , the position of the leader robot for  $k > k_2$  is predicted by

$$\begin{cases} \hat{x}_l(t_k) = \hat{x}_l(t_{k-1}) + v_0 T_s \cos \hat{\theta}_l(t_k) \\ \hat{y}_l(t_k) = \hat{y}_l(t_{k-1}) + v_0 T_s \sin \hat{\theta}_l(t_k) \\ \hat{\theta}_l(t_k) = \hat{\theta}_l(t_{k2-1}) \end{cases} \tag{6}$$

**5) N-r-mode:** After avoiding the obstacle, the follower robot has to re-construct the original formation shape. *Position Approach* in N-r-mode manages the process of the re-construction. First, the target point for constructing the original shape, denoted as  $P(x_p, y_p)$ , is defined. The follower robot is then controlled so as to move toward the target point. As an example, consider a case that the original formation shape of  $F_1$  is *Triangle* as shown in Fig. 4(a), while the formation shape for obstacle avoidance is *Line*, and the mode is changed to N-r-mode. Then, the target point of  $F_1$  is given by

$$\begin{cases} x_p(t_{k3}) = x_{f1}(t_{k3}) + \sqrt{2} d_{f1}(t_{k3}) \cos \{ \theta_{f1}(t_{k3}) - \frac{\pi}{4} \} \\ y_p(t_{k3}) = y_{f1}(t_{k3}) + \sqrt{2} d_{f1}(t_{k3}) \sin \{ \theta_{f1}(t_{k3}) - \frac{\pi}{4} \} \end{cases} \tag{7}$$

where  $(x_{f1}, y_{f1}, \theta_{f1})$  are the states of  $F_1$  and  $d_{f1}$  is the relative distance. Equation (7) means that the target point is given to make a right-angled isosceles triangle with positions of  $F_1$  and  $F_2$  at  $t_{k3}$ . It is necessary to update the target point with progress of the time. Supposing that  $L$  moves toward the goal with the normal linear velocity  $v_0$ ,  $(x_p, y_p)$  for  $k > k_3$  are updated by

$$\begin{cases} x_p(t_k) = x_p(t_{k-1}) + v_0 T_s \cos \theta_p(t_k) \\ y_p(t_k) = y_p(t_{k-1}) + v_0 T_s \sin \theta_p(t_k) \\ \theta_p(t_k) \square \tan^{-1} \frac{y_g - y_p(t_{k3})}{x_g - x_p(t_{k3})} \end{cases} \tag{8}$$

where  $(x_g, y_g)$  are the goal coordinates of  $L$ . Furthermore, since the leader of  $F_1$  after re-construction is changed to  $L$  from  $F_2$ , it is necessary that the estimated position of the leader robot is changed as

$$\begin{cases} \hat{x}_l(t_{k3}) = \hat{x}_l(t_{k3-1}) + d_{f1}^{ref} \cos \{ \theta_p(t_{k3}) + \gamma_{f1}^{ref} \} \\ \hat{y}_l(t_{k3}) = \hat{y}_l(t_{k3-1}) + d_{f1}^{ref} \sin \{ \theta_p(t_{k3}) + \gamma_{f1}^{ref} \} \end{cases} \tag{9}$$

where  $d_{f_1}^{ref}$  and  $\gamma_{f_1}^{ref}$  are the references of the relative distance and the relative angle of  $F_1$ , respectively. After  $F_1$  reached near the target point, the mode is changed to N-f-mode from N-r-mode. The re-construction is succeeded if  $F_1$  detected and tracked  $L$  again.

#### IV. EXPERIMENTS OF FORMATION CONTROL

This section presents an experimental result using three mobile robots; two Pioneer-1 and one Pioneer-2, to demonstrate the effectiveness of the proposed navigation techniques. The leader robot is denoted as  $L$ , while the two follower robots are denoted as  $F_1$  and  $F_2$  also in this section. The formation shape for formation control was given by *Triangle*, while the one for obstacle avoidance was *Line*. Their referenced relative distance and angle were given as follows.

➤ *Triangle* (shape=73)

$$d_{f_1}^{ref} = 600 \text{ [mm]}, \gamma_{f_1}^{ref} = 15 \text{ [deg]} \quad \text{for } F_1$$

$$d_{f_2}^{ref} = 600 \text{ [mm]}, \gamma_{f_2}^{ref} = -30 \text{ [deg]} \quad \text{for } F_2$$

➤ *Line* (shape=71)

$$d_{f_1}^{ref} = 600 \text{ [mm]}, \gamma_{f_1}^{ref} = 0 \text{ [deg]} \quad \text{for } F_1$$

$$d_{f_2}^{ref} = 600 \text{ [mm]}, \gamma_{f_2}^{ref} = 0 \text{ [deg]} \quad \text{for } F_2$$

The formation velocity and the maximum command inputs were given by  $v_0 = 100 \text{ [mm/s]}$ ,  $v_{max} = 200 \text{ [mm/s]}$  and  $\omega_{max} = 6 \text{ [rad/s]}$ . The sampling time was given by  $T_s = 0.1 \text{ [s]}$ .

The experimental result of the formation control with a large obstacle is shown in Fig. 6 - 10. In Figs. 6 and 7, the solid-lines indicate traces of  $L$ ,  $F_1$  and  $F_2$ . The dashed-lines indicate traces of leader position estimated by both  $F_1$  and  $F_2$ , respectively. The origin of the Cartesian coordinates was placed at the start point of  $L$ . The goal of  $L$  was located at  $(6000, 0) \text{ [mm]}$ . The positions of robots were obtained by deadreckoning of the robots. The accumulated error on the positions was less than a few centimeters in the experiment since the travel distance of the robots in the experiment was not so long.  $F_1$  and  $F_2$  were placed to make a triangle at start. The experiment was therefore started with supposing that an object detecting by  $F_1$  and  $F_2$  during a few initial seconds was  $L$ . An ellipsoidal obstacle was placed on the way between start and goal. The size was approximately  $1300 \times 800 \text{ [mm]}$ . The upper and the lower of Fig. 8 respectively show the time histories of the flag number and the formation shape of  $F_1$  and  $F_2$  where the mode flag numbers are listed in Table II. Figures 9 and 10 are the relative distance and angle of  $F_1$ , where  $d_{f_1}$  and  $\gamma_{f_1}$  were obtained the Eq. (3), and  $d_{f_1}^*$  and  $\gamma_{f_1}^*$  were true relative distance and the true relative angle.

After  $L$  avoided the obstacle,  $F_1$  encountered the obstacle. According to the judgement of *Form Change*, the formation shape of  $F_1$  was changed to *Line* (shape=71) at  $t=17.2 \text{ [s]}$  and its leader robot was changed from  $L$  to  $F_2$  (Fig. 8). The locations of  $L$ ,  $F_1$  and  $F_2$  in this time are marked by the black, blue and red asterisks in Figs. 6 and 7, respectively. The leader position estimated by  $F_1$ , drawn by the cyan dashed-line, was shifted to the trace of  $F_2$  as shown in Figs. 6 and 7. At  $t=40.0 \text{ [s]}$ , the distance from  $F_1$  to the obstacle was longer than a threshold. Then, the mode of  $F_1$  was selected as N-r-mode (flag=18), the re-construction of the formation shape in  $F_1$  began; that is,  $t_{k3}=40.0 \text{ [s]}$ . The locations of  $L$ ,  $F_1$  and  $F_2$  at this time are marked by the black, blue and red triangles in Figs. 6 and 7, respectively. The leader robot of  $F_1$  after re-construction was returned to  $L$ . Then using Eq. (9), the leader position estimated by  $F_1$  was changed from the position marked by the red-edged cyan triangle ( $t_{k3-1}=39.9 \text{ [s]}$ ) to the one marked by the black-edged cyan triangle ( $t_{k3}=40.0 \text{ [s]}$ ) in Fig. 6. Comparing the cyan-triangles to the red and the black triangles in Fig. 6, it is seen that these estimated leader positions were properly estimated. The target position of  $F_1$  for re-constructing the triangle formation shape was calculated by Eq. (7) at the position marked by the green triangle.  $F_1$  then moved the targeted position with the maximum linear velocity. The target position was also updated by Eq. (8) toward to the goal with the normal linear velocity. The re-construction was finished at  $t=49.4 \text{ [s]}$ . The locations of  $L$ ,  $F_1$  and  $F_2$  at this time are marked by the black, blue and red circles in Fig. 6. The original formation shape *Triangle* was re-constructed since  $F_1$  detected  $L$  again after that. As explained so far, the proposed techniques were effective in the formation control with the large obstacle avoidance.

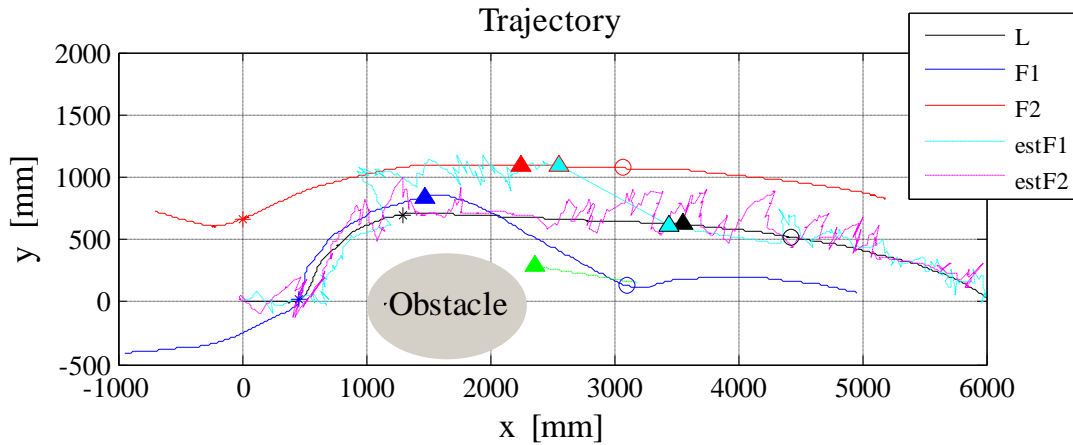


Figure 6: Traces of  $L$ ,  $F_1$  and  $F_2$  and traces of leader position estimated by  $L$ ,  $F_1$  and  $F_2$

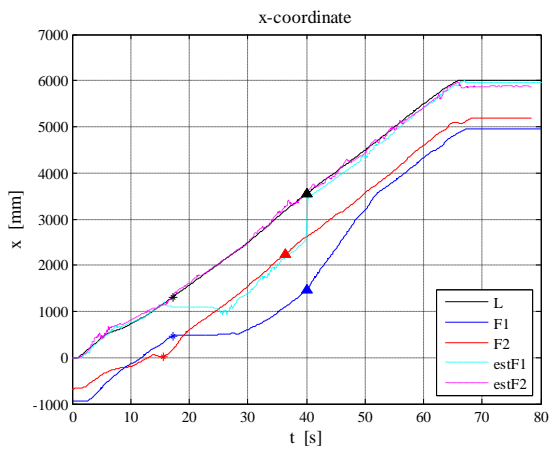


Figure 7: Time histories of  $x$ -coordinate;  $x_i(t)$ ,  $x_{f1}(t)$ ,  $x_{f2}(t)$  (drawn by solid-lines) and  $\hat{x}_i(t)$  (drawn by dashed-lines) estimated by  $F_1$  and  $F_2$

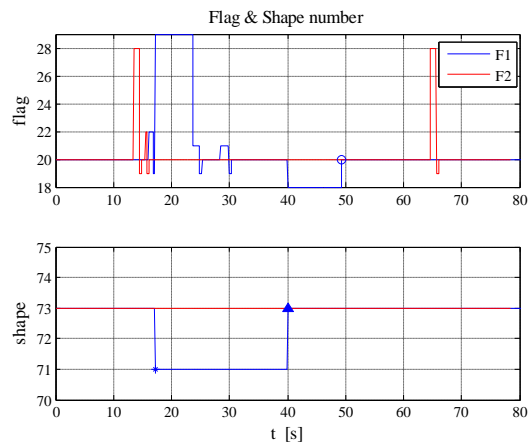
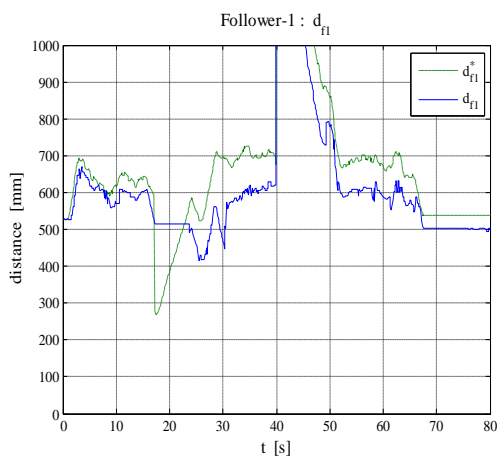


Figure 8: Time histories of mode flag and formation shape

Table II: Flag number and mode

flag number	mode	flag number	mode
18	N-r-mode	24	Left in A-mode
19	N-s-mode	25	Left-Right in A-mode
20	N-f-mode	26	Front-Left in A-mode
21	Right in A-mode	27	Left-Front-Right in A-mode
22	Front in A-mode	28	Back in A-mode
23	Front-Right in A-mode		





**Figure 9: Time histories of relative distance  $d_{f1}$**

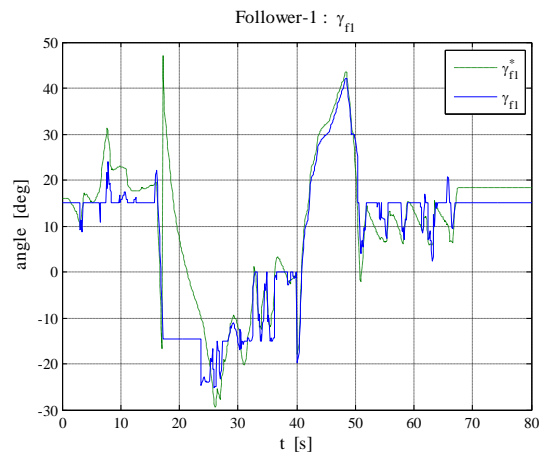


**Figure 10: Time histories of relative angle  $\gamma_{f1}$**

### V. CONCLUDING REMARKS

This paper has presented a formation control of multiple mobile robots with large obstacle avoidance. The mobile robots considered in this paper had multiple sonars which were used for not only constructing formation but also avoiding obstacle. Based on the techniques [12], some novel modules were introduced to accomplish the obstacle avoidance and formation control. The effectiveness of the proposed techniques was examined by an experiment using three mobile robots.

### REFERENCES

- [1]. Jaydev P. Desai, James P. Ostrowski and Vijay Kumar, "Modeling and control of formations of nonholonomic mobile robots," IEEE Transactions on Robotics and Automation, Vol. 17, No. 6, pp. 905-908, December 2001.
- [2]. Aavek K. Das, Rafael Fierro, Vijay Kumar, James P. Ostrowski, John Spletzer, and Camillo J. Taylor, "A vision-based formation control framework," IEEE Transactions on Robotics and Automation, Vol. 18, No. 5, pp. 813-825, October 2002.
- [3]. Luca Consolini, Fabio Morbidi, Domentico Prattichizzo, and Mario Tosques, "Leader-follower formation control of nonholonomic mobile robots with input constraints," Automatica, Vol. 44, No. 5, pp. 1343-1349, May 2008.
- [4]. Herbert G. Tanner, George J. Pappas, and Vijay Kumar, "Leader-to-formation stability," IEEE Transactions on Robotics and Automation, Vol. 20, No. 3, pp. 443-455, June 2004.
- [5]. Jin B. Park Bong S. Park and Yoon H. Choi, "Adaptive formation control of electrically driven nonholonomic mobile robots with limited information," IEEE Transactions on Systems, Man and Cybernetics Part B, Vol. 41, No. 4, pp. 1061-1075, August 2011.
- [6]. Tucker Balch and Ronald C. Arkin, "Behavior-based formation control for multi-robotic teams," IEEE Transactions on Robotics and Automation, Vol. 14, No. 6, pp. 926-934, December 1998.
- [7]. A. Rizzi R. Burrige and D. Koditschek, "Sequential composition of dynamically dexterous robot behavior," The International Journal of Robotics Research, Vol. 18, pp. 926-934, June 1999.
- [8]. Kar-Han Tan and Anthony M. Lewis, "Virtual structures for high precision cooperative mobile robot control," Proc. of IEEE/RSSJ International Conference on Intelligent Robots and Systems, Volume 3, pp. 132-139, November 1996.
- [9]. Atsushi Fujimori, Takeshi Fujimoto, and Gábor Bohács, "Formatted navigation of mobile robots using distributed leader-follower control," Proc of 16th IFAC World Congress, Prague, Czech Republic, July 2005.
- [10]. Atsushi Fujimori, Tomoya Saito, and Gábor Bohács, "Formatted navigation of mobile robots with obstacle avoidance. In IEEE Conference on Robotics, Automation and Mechatronics. Budapest, Hungary, June 2006.
- [11]. Atsushi Fujimori, Takeshi Fujimoto, and Gábor Bohács, "Mobile robot formation control using a modified leader-follower technique," Integrated Computer-Aided Engineering, Vol. 15, No. 1, pp. 71-84, January 2008.
- [12]. Atsushi Fujimori, Hiroshi Kubota, Naoya Shibata, and Yoshinari Tezuka, "Leader-follower formation control with obstacle avoidance using sonar-equipped mobile robots," Journal of Systems and Control Engineering, Vol. 228, No. 5, pp. 303-315, 2014.
- [13]. Inc. ActivMedia. Pioneer 1 Operations Manual, 1996.
- [14]. Inc. ActivMedia. Pioneer-1 Software Manual, Version 4.1.2, 1996.
- [15]. Inc. ActivMedia. Pioneer 2 Operations Manual, Version 2, 2003.

Atsushi Fujimori "A Modified Navigation Technique for Formation Control of Sonar-Equipped Mobile Robots with Large Obstacle Avoidance" International Journal of Modern Engineering Research (IJMER), vol. 08, no. 11, 2018, pp 44-52